

## Forest cover classification using Landsat Thematic Mapper data for areal expansion of line LAI estimate generated through airborne laser profiler

Naoko Sasaki, Kiyoshi Takejima, Tomoko Kusakabe\* and Tatsuo Sweda

*College of Agriculture, Ehime University, 3-5-7 Tarumi, Matsuyama 790-8566*

**Abstract:** A simple cover classification of Canadian boreal forest was conducted using Landsat Thematic Mapper (TM) imagery to expand a line estimate of leaf area index (LAI) into a two-dimensional regional one. The line estimate had been made through a 600 km long continuous vegetation profile obtained by airborne laser altimetry. The present study area of  $170 \times 30$  km straddles the central portion of the laser profiling transect, from Wandering River north to Fort McMurray, Alberta, Canada. A total of eight land cover types were identified first in the field, and then some 83 training points and another 74 reference points were chosen and recorded for a supervised classification and its accuracy assessment respectively. By applying a supervised procedure to Landsat TM data in two different seasons, these eight cover types, consisting of six vegetated covers, *i.e.* closed and open conifer forests, conifer woodland, closed and open broad-leaved forests and marsh thicket, and two non-vegetated covers, *i.e.* bare ground and water surface, were classified. The classification was basically successful with an overall accuracy of 76%. Finally, using an overlay of this land cover map and the airborne laser profiling flight track, the mean LAI for each type of vegetation cover was obtained, and subsequently fed back to the land cover map to form a false-color map showing the two-dimensional distribution of LAI over the entire study area.

**key words:** Landsat TM, land cover classification, airborne laser altimetry (ALA), boreal forest, Canada

### Introduction

Estimating reliable leaf area index (LAI) on a regional or larger scale has become an urgent task for global warming research because LAI is one of the critical boundary conditions in general circulation models, a major tool for studying future climate changes (Mabuchi *et al.*, 1997; Sellers, 1992). LAI is also a key biological indicator for monitoring possible vegetation change due to global warming. This is especially true in higher latitudes where the present work was conducted since quantitative changes in LAI or biomass are expected to precede qualitative change in species composition, *i.e.* vegetation change. In our recent work (Kusakabe *et al.*, 2000), we have applied airborne laser altimetry for expedient estimation of LAI, and obtained a 600 km long line estimate of LAI along a flight track extending from Edmonton, Alberta to Cluff Lake, Saskatchewan in the Canadian boreal forest. In the present study, the possibility of simple vegetation cover classification with satellite radiometer imagery was investigated to expand the line estimate of LAI to a two-dimensional regional one. Use

\* E-mail address: kusa@agr.ehime-u.ac.jp

of satellite data for vegetation cover classification itself is commonplace. It is found especially useful for the boreal region partly because of its expanse and inaccessibility and partly because of the relative ease in applying satellite data to relatively simple vegetation cover characterizing to the region. Accordingly many vegetation cover classification works have been conducted with various algorithms in a multitude of spatial scales and class designations (Cihlar *et al.*, 1997; Nelson, 1984; Shen, 1985; Steyaert *et al.*, 1997). In our vegetation cover classification, emphasis was placed on developing a simple and efficient classifier to discriminate at least between conifer and broad-leaved forest stands for Landsat Thematic Mapper (TM) data. The distinction between conifer and broad-leaved forests is crucial here since in the laser profiling estimate, where LAI was obtained from standing stock of stem biomass, the LAI for given standing stock was significantly different between conifer and broad-leaved species, while it was rather negligible within each group (Kusakabe *et al.*, 2000). Thus in the present work, we used supervised decision tree classifier for its intuitive simplicity, flexibility and computational efficiency (Friedl and Brodley, 1997). In the two dimensional expansion of line estimate of LAI, the simplest method of relating line LAI estimates to the vegetation classification was adopted primarily to demonstrate the possibility of such expansion.

### Materials and methods

#### Study area

For the present study, we selected a  $170 \times 30$  km area between Wandering River and Fort McMurray, Alberta, Canada (Fig. 1). This area is in the boreal forest zone (Barbour and Billings, 2000), and constitutes lengthwise the central one third of our original laser profiling transect along which the latitudinal distributions of standing stock (Tsuzuki *et al.*, 1998) and LAI (Kusakabe *et al.*, 2000) were estimated. Except for steep gorges, the area is gently rolling with the highest and lowest elevations respectively at 750 m and 400 m above sea level, and drains northward eventually to the Arctic Ocean via the Athabasca River and its intricate system of tributaries. Mean annual temperature and annual precipitation at Fort McMurray, the northern end of the study area, are  $0.0^{\circ}\text{C}$  and 445.8 mm, respectively (National Climatic Data Center, NOAA). The growing season, when the mean monthly temperature rises above  $5^{\circ}\text{C}$ , is May to September. This region is characterized by extensive and frequent fires during the dry summer months, resulting in large patches of primarily even-aged single-species stands of black spruce (*Picea mariana*), white spruce (*Picea glauca*), jack pine (*Pinus banksiana*) and trembling aspen (*Populus tremuloides*) regenerated after fires. The vertical structure of forest stands is simple with a single canopy layer except for some aspen stands and old stands of tall timber species. In some cases in aspen stands, simultaneously-regenerated after fire but slow-growing spruce constitutes a loose second canopy layer. In old stands which are rather rare because of frequently recurring fires, gap regeneration makes canopy structure rugged and uneven. Forest floor vegetation is rather poor with such species as bearberry (*Arctostaphylos uva-ursi*), prickly rose (*Rosa acicularis*), blueberry (*Vaccinium myrtilloides*) and reindeer lichen (*Cladina* spp.) at dry sites where the canopy is dominated by jack pine, Labrador tea (*Ledum*

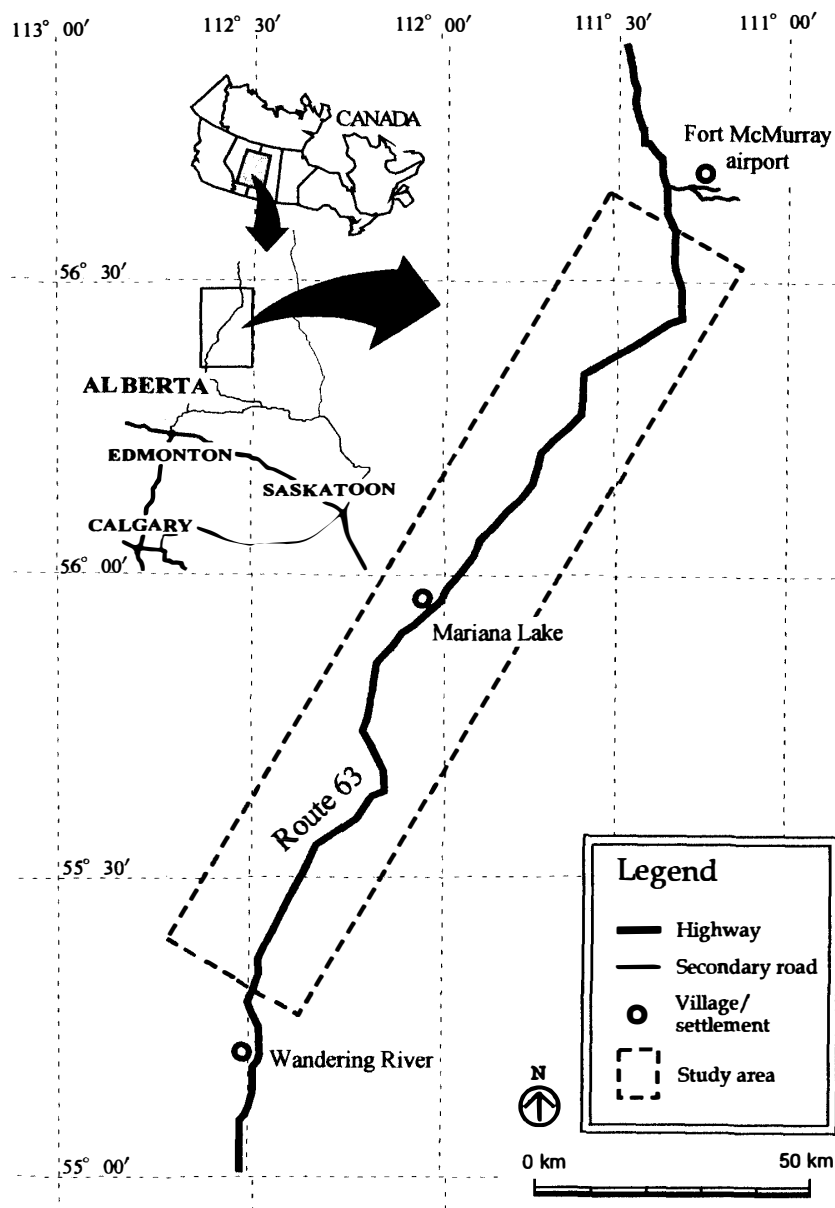


Fig. 1. Location of the 170 × 30 km study area in northern Alberta.

*groenlandicum*), cranberry (*Vaccinium* spp.) and horsetail (*Equisetum* spp.) in mesic sites under the canopy of aspen, white spruce and/or black spruce, and Labrador tea and peat moss (*Sphagnum* spp.) in wet black spruce woodland.

#### Field survey and land cover types

In the former half of the field survey conducted in August and September 1999, vegetation cover types were identified on the ground through a meticulous comparison between field observation and false-colored composite of Landsat TM imagery tentatively prepared for this purpose. Based primarily on canopy tree species and physiognomic features, a total of six vegetation cover types were established as in Table 1. The most important criterion in this cover type classification was distinction

Table 1. Land cover types used for classification.

Land cover types	Dominant species	Canopy closure	Canopy height
Closed conifer forest	<i>Picea glauca</i> <i>Picea mariana</i> <i>Pinus banksiana</i>	closed	tall
Open conifer forest	<i>Pinus banksiana</i>	open	short
Conifer woodland	<i>Picea mariana</i>	open	tall
Closed broad-leaved forest	<i>Populus tremuloides</i>	closed	tall
Open broad-leaved forest	<i>Populus tremuloides</i>	open	short
Marsh thicket	<i>Alnus</i> spp. <i>Salix</i> spp. <i>Betula</i> spp.	closed	short-intermediate
Bare ground	–	–	–
Water	–	–	–

between conifer and broad-leaved species, since in the laser profiling estimate, when LAI was regressed upon canopy profile via standing stock, the LAI for a given standing stock was significantly different between conifer and broad-leaved species (Kusakabe *et al.*, 2000). Thus the closed conifer forest category in Table 1 includes those of black spruce, white spruce and jack pine, whereas the closed broad-leaved forest indicates that of aspen, the sole dominant broad-leaved timber species in the study area.

The other criterion in the vegetation cover type classification was the state of canopy closure since it may well affect the spectral reflectance in the Landsat TM imagery. Accordingly, three open forest types were established as in Table 1. The open conifer forest designates only sparsely-growing jack pine stands in the sapling stage shortly after fires. The conifer woodland means stands of stunted black spruce growing sparsely. Again, aspen being the sole dominant broad-leaved timber species, the open broad-leaved forest indicates sparsely-growing aspen stands in the sapling stage. In addition to these five vegetation types, the marsh thicket, where willow (*Salix* spp.), birch (*Betula* spp.) and alder (*Alnus* spp.) grow mixed, was recognized, making a total of six vegetated land cover types. Marshes, fens, meadows and peat bogs, where trees are short or scarce, are included in the marsh thicket category for simplicity. In addition to these, bare ground and water surface were recognized as separate land cover types, thus resulting in a total of eight cover types altogether.

Then in the latter half of the field survey, the distribution of these eight land cover types was mapped on 1:250000 topographic maps. The mapping was conducted primarily on the ground, in which boundaries between different cover types were demarcated along the highway. Then, these boundaries were extended away from the highway by observation from aircraft flown particularly for this purpose twice over the entire length of the study area, respectively 500 m and 150 m above ground.

While mapping, we also noted canopy species composition, status of canopy closure (closed or open) and canopy height class (tall, intermediate, or short). Only the canopy species were identified and recorded because the spectral reflectance is influenced primarily by the canopy layer, and the vertical structure of foliage in the forests was

simple and canopy trees dictated LAI in the majority of cases. In this process of vegetation mapping, a score or so typical forest stands for each cover type were identified on the ground, in which plots were set up and their exact location was recorded on 1:250000 topographic maps for use as training data for supervised classification of the Landsat TM imagery as well as reference data for assessing the classification accuracy. Both the training and reference plots were located at the most representative sites toward the center of these large tracts of stands. Exception to this choice of training/reference plots were the bare ground, water body and marsh thicket. The former two are readily identifiable even in the Landsat TM imagery. On the other hand, large expanses of marsh thicket were difficult to find since the highway, along which the training/reference plots were located, is constructed along the raised topography.

#### Supervised land cover classification

Landsat TM is one of sensors used for land cover classification, and has been used for various vegetation classification studies (Bolstad and Lillesand, 1992; Cohen and Spies, 1992; Fox *et al.*, 1983; Moore and Bauer, 1990; Wolter *et al.*, 1995). Among such other sensors as Landsat Multispectral Scanner (MSS), SPOT High Resolution Visible (HRV) and NOAA Advanced Very High Resolution Radiometer (AVHRR), we selected Landsat TM because it has finer spatial resolution of 30 m (except band 6 (120 m)) than MSS, and is multi-spectral with seven bands covering from visible to thermal infrared (U.S. Geological Survey and NOAA, 1984). For detecting the seasonal difference in spectral radiance, two scenes of different seasons, but covering the same area (Path 42, Row 21), *i.e.* one captured in the spring (May 11, 1998) and the other in the fall (September 24, 1995), were used. It is preferable to use data of the same year, but haze and cloud cover prevented this. Out of each original scene of 185 × 170 km coverage on the ground, a 170 × 30 km area was cut out for the present study. Geometrical distortion in the Landsat TM imagery was corrected using twenty-one ground control points located in the 1:250000 topographic maps.

For identifying spectral radiance characteristics of each land cover type, the training points mentioned in the preceding section were used. At each training point, 5 × 5 pixels were extracted as training data. Numbers of these training points and training pixels for each land cover type are given in Table 2.

To establish a decision tree according to which the land cover type classification is to be conducted, a total of 17 radiance attributes were examined, of which 14 were single numerical descriptors and the remaining three were composite. A single descriptor is simply a digital number, or radiance in  $2^8 = 256$  radiometric resolution for each of the seven bands of the two different seasons. One of the composite descriptors is the normalized difference vegetation index (NDVI), which is defined as

$$\text{NDVI} = (\text{NIR} - \text{R}) / (\text{NIR} + \text{R}),$$

where NIR and R represent, respectively, near-infrared and red radiances. Because green leaves have high reflectance in infrared and low in red, NDVI can effectively distinguish vegetated area from other areas (*e.g.* Barrett and Curtis, 1992). More specifically in our case, bands 4 and 3 correspond to NIR and R, and NDVI was

Table 2. Training data sets for supervised land cover classification.

Land cover types	Number of plots	Number of pixels
Closed conifer forest	10	250
Open conifer forest	11	275
Conifer woodland	7	150
Closed broad-leaved forest	21	525
Open broad-leaved forest	23	575
Marsh thicket	4	100
Bare ground	5	169
Water	2	50

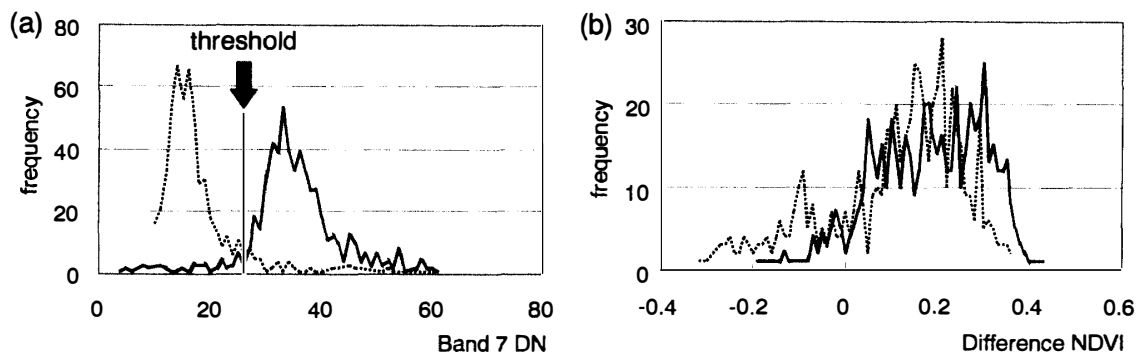


Fig. 2. Examination of class signatures and threshold. Frequency distributions of (a) Band 7 digital number and (b) seasonal difference NDVI for closed (----) and open (—) broad-leaved forests.

computed as

$$\text{NDVI} = (\text{DN4} - \text{DN3}) / (\text{DN4} + \text{DN3}),$$

where DN3 and DN4 are digital numbers in bands 3 and 4, representing relative radiance at  $2^8 = 256$  tone levels respectively. Two NDVIs are involved here, *i.e.* one for the spring scene and the other for the fall. The last composite descriptor is the difference NDVI, which is calculated as the difference between the spring and fall NDVIs.

To find the most sensitive numerical descriptor to discriminate one cover type from another, frequency distributions of the descriptor values by cover type were examined, as shown in Fig. 2. In this figure, distributions of band 7 digital number and the difference NDVI are shown respectively as the sensitive (a) and insensitive (b) cases to distinguish between closed broad-leaved forests and open broad-leaved forests.

Once the specific descriptors most appropriate for discrimination were identified, fine-tuning of the threshold was conducted iteratively until the optimum accuracy of classification was achieved. The resultant decision tree classifier is shown in Fig. 3.

#### Application of the decision tree classifier and accuracy assessment

All pixels within the  $170 \times 30$  km study area were classified using the decision tree

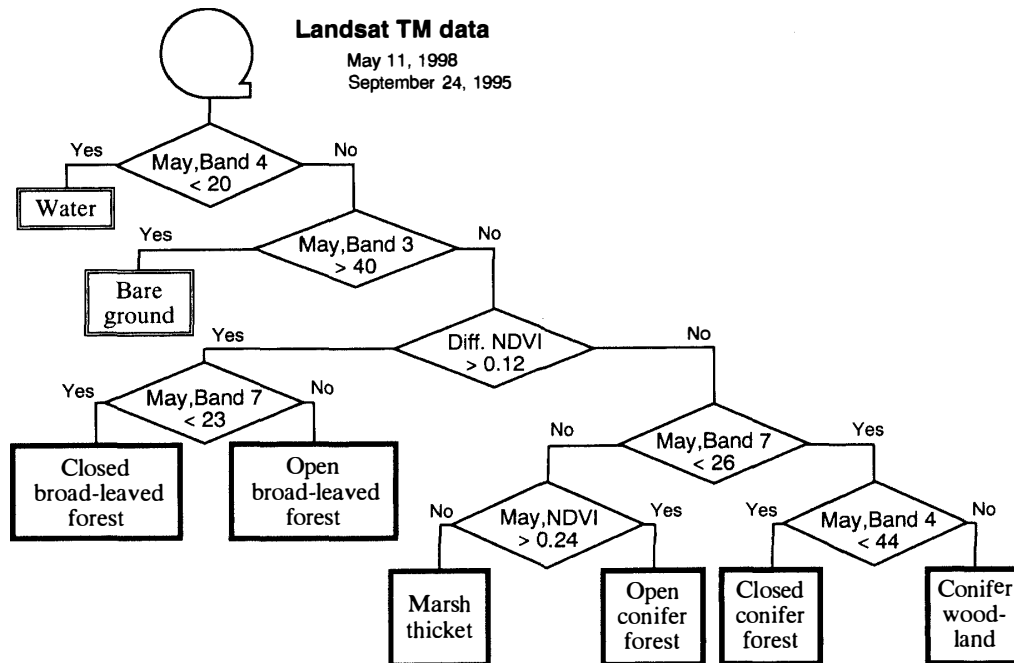


Fig. 3. Decision tree for land cover type classification.

and colored to produce a land cover map. Subsequently, the accuracy of classification was assessed using the reference data set, completely independent of the training data set. Here, a total of 74 reference areas representing a total of 3215 pixels on the Landsat TM imagery are involved. Unlike the training areas, the reference areas were irregular in shape.

In assessing the classification accuracy, two types of errors, *i.e.* Type I and II errors, were considered. A Type I error is one in which a pixel of type A is classified as non-A, whereas a Type II error is one in which a non-A pixel is classified as A. The degree of freedom from Type I error, hereafter referred to as producer's accuracy, was calculated as the percentage of correctly-classified pixels to the number of pixels of the same class in the original reference data. Similarly, freedom from Type II error, referred to as user's accuracy, is the percentage of correctly-classified pixels to the total number of pixels classified as the same kind (Lillesand and Kiefer, 1994).

#### Areal expansion of line LAI estimate

Based on the vegetation map produced in the preceding section, the line estimate of LAI obtained through airborne laser altimetry of the vegetation profile (Kusakabe *et al.*, 2000) was expanded two-dimensionally. In principle the line estimate of LAI, shown in Fig. 4, was obtained as follows:

The direct product of the airborne laser altimetry was the vegetation profile, with horizontal resolution of 50 cm along the flight track in our case. A correlation analysis of 14 ground truth sample plots revealed that the area under the vegetation profile was proportional to the standing biomass, which in turn was well correlated with LAI. Thus, by establishing two regressions, one of LAI upon standing biomass, and the other of standing biomass upon vegetation profile, and then applying them to the vegetation

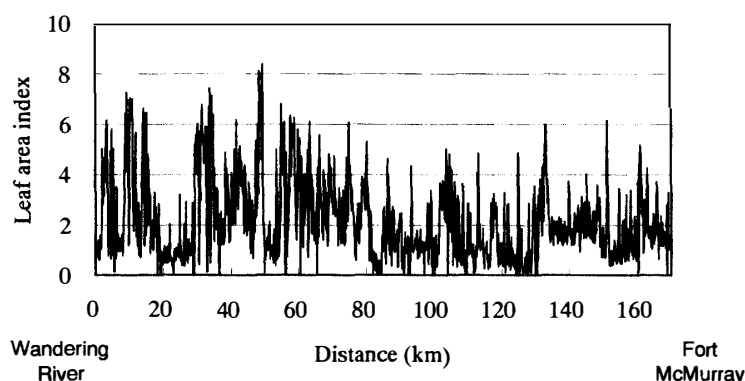


Fig. 4. Line estimate (latitudinal distribution) of LAI as evaluated from vegetation profile captured with airborne laser altimetry system (Partly redrawn from Kusakabe *et al.*, 2000).

profile, the line estimate of LAI given in Fig. 4 was obtained (Kusakabe *et al.*, 2000).

Of conceivable methods to expand Fig. 4 two-dimensionally to an areal estimate of LAI, the simplest approach was taken in the present work, primarily to demonstrate the possibility. To begin with, the continuous line estimate of LAI was segmented into the eight land cover types using an overlay of the Landsat cover type map (Fig. 5) and the airborne laser altimetry flight track. Then the mean LAI was calculated for each vegetation type, which turned out to be 3.46 for closed conifer forest, 1.01 for open conifer forest, 1.60 for conifer woodland, 3.06 for closed broad-leaved forest, 0.97 for open broad-leaved forest and 0.86 for marsh thicket, and then fed back to the land cover map by pixel to result in the false color LAI map shown in Fig. 6.

### Results and discussion

Classification of the Landsat TM imagery with our decision tree classifier resulted in the land cover type map shown in Fig. 5. The overall accuracy for eight land cover types, calculated as the ratio of all the correctly classified pixels to the total number of pixels used for assessment was 76% (Table 3). The supervised classification procedure worked reasonably well for five land cover types, *i.e.* for closed conifer forest (user's accuracy of 81% and producer's accuracy of 81%), closed broad-leaved forest (76% and 98%), open broad-leaved forest (93% and 79%), bare ground (100% and 100%) and water surface (100% and 100%). Open conifer forest revealed relatively high user's accuracy (67%), but was poor in producer's accuracy, *i.e.* of 576 original pixels only 264 were correctly classified as such resulting in producer's accuracy of 46%. In contrast, conifer woodland revealed high producer's accuracy (86%) and low user's accuracy (59%). The decision tree worked poorly both ways for marsh thicket (26% user's and 19% producer's).

As has been overviewed above, marsh thicket revealed the poorest performance both in user's and producer's accuracies. Of several conceivable causes, the most directly responsible would be the open nature of the canopy structure. The spectral reflectance of open forests comes partially from the canopy and partially from the ground, be it water, soil or ground vegetation, with the proportion of each depending



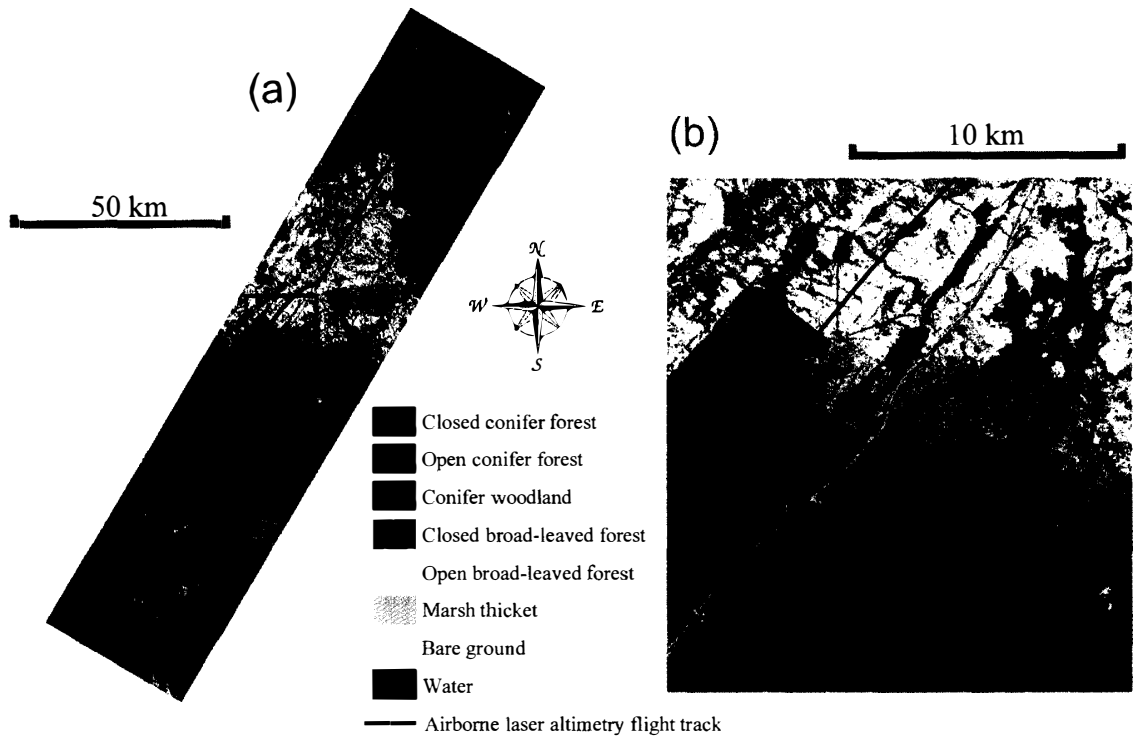


Fig. 5. Land cover map of the entire study area (a) and blowup of its portion (b).

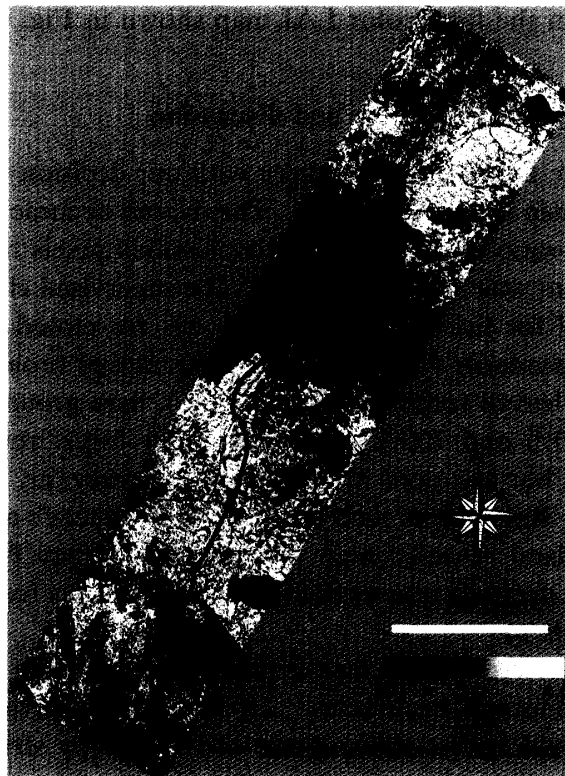


Fig. 6. Spatial distribution of LAI.

Table 3. Error matrix for eight land cover types.

Classified data*	Reference data*								Row total	User's accuracy (%)
	CC	OC	CW	CB	OB	MT	BG	W		
CC	407	31	14	2	5	42	0	0	501	81
OC	0	264	0	0	61	70	0	0	395	67
CW	23	242	406	4	6	6	0	0	687	59
CB	71	0	51	397	0	0	0	0	519	76
OB	0	33	0	1	578	12	0	0	624	93
MT	0	6	0	0	80	31	0	0	117	26
BG	0	0	0	0	0	0	71	0	71	100
W	0	0	0	0	0	0	0	301	301	100
Column Total	501	576	471	404	730	161	71	301	3215	
Producer's accuracy (%)	81	46	86	98	79	19	100	100		
Overall accuracy	76 %									

\* CC, closed conifer forest; OC, open conifer forest; CW, conifer woodland; CB, closed broad-leaved forest; OB, open broad-leaved forest; MT, marsh thicket; BG, bare ground; W, water.

upon the openness of the canopy as well as the composition of the ground cover. This reduces the influence of the canopy reflectance on the classification and increases the possibility of misclassification. The same is true with other types of open forests, all of which revealed relatively poorer producer's accuracy than did the closed forests.

Next responsible would be the choice of training area in the field. With roads constructed through relatively dry upland, extensive marsh thickets were difficult to reach. This resulted in placing training/reference plots in relatively small expanses of marsh thickets, in which case the classification accuracy deteriorates drastically when exact correspondence happens to fail between the actual training/reference plots and the Landsat TM imagery pixels. The other methodological problem would be the way the decision tree was constructed. In the present work, the best but only one criterion was used at each decision branch. Use of multiple criteria instead may well improve the accuracy. The sequence of criteria may also affect accuracy, but it was arranged more or less intuitively in the present work.

There are other causes of misclassification applicable not only to the marsh thicket but also to the other cover types. One is the choice of Landsat data which includes choice of year and season. We used seasonally-differential NDVI to distinguish conifer from broad-leaved forest. In this case, the best discrimination between conifer and broad-leaved forest can be made from a set consisting of a spring scene taken when deciduous leaves are fully developed and a fall scene taken when they are completely gone. Our Landsat data set nearly fulfills this condition but not fully, thus resulting in some misclassification. The combination of bi-seasonal data of different years in this work may also constitute an additional source of classification error. The last possible source of error could be the fall scene of 1995 taken immediately after a major fire, the haze from which might have altered the total radiance by adding significant scattered extraneous path radiance.

Figure 6 shows the areal distribution of LAI. Darker colors represent lower LAI and lighter colors higher LAI. Black areas represent water body and bare ground where LAI is nil. LAI is significantly lower in the dark reddish stretch occupying the third quarter from the bottom of the study area. It is a burn from a recent (1995) major fire, and the vegetation is just returning. The overall mean LAI of the entire study area turned out to be 2.19.

This overall areal mean is significantly smaller than the simple arithmetic mean of plot LAI estimates which has often been cited as that for boreal forest region in general (*e.g.* Whittaker and Likens, 1975). Our plot LAIs, measured in 14 plots and constituted the basis of the line estimate, and thus consequently the areal estimate in the present work, ranged from 0.54 to 6.22 with a simple arithmetic mean of 2.40. This difference of 0.21 between the plot mean and the areal mean of 2.19 is clearly a systematic deviation associated with scaling-up from plot values to a regional mean.

More specifically, there are three factors involved in this systematic deviation. The first is water bodies and bare lands which together occupy some 3% of the study area. These land cover types are never chosen for plot measurement of LAI but are included in the regional mean LAI. The second factor is the effect of recent burn where tiny seedlings were just returning. Such fresh burns were neither represented in our sample plots nor in other LAI studies on boreal forest (Cannell, 1982; Chen *et al.*, 1997), but they constitute a considerable portion of the boreal forest zone. The third factor is the underrepresentation in our sample plots of less typical types of vegetation cover such as marsh thicket, conifer woodland and open conifer and broad-leaved forests. Though they cover a considerable portion of the boreal zone, they are not what is generally regarded as typical boreal forest and thus underrepresented in our LAI ground truth sample plots. This result clearly indicates that the regional mean LAI cannot be probably represented by spot values obtained in general by measuring sample plots established in stands of vegetation typical of the ecotone they are supposed to represent.

On the other hand, the overall mean of 2.14 for the line estimate of LAI (Kusakabe *et al.*, 2000) is not as different from the overall areal mean of 2.19. Judging from this small discrepancy and even inversed direction of change, this difference is considered as random fluctuation in a line sample of airborne laser altimetry taken lengthwise from the rectangular study area in which the overwhelming environmental gradient also runs lengthwise, *i.e.* north-south. Although more case studies are needed for a more decisive conclusion, our result suggests that areal expansion of LAI from the line estimate may not be as rewarding as line expansion from the plot estimates in accessing the true LAI for the boreal forest region.

The strength of the airborne laser altimetry exists in its capacity to retrieve canopy height information continuously, but with the weakness of one-dimensional line coverage along the flight track. Conversely, the strength of satellite radiometer imagery exists in its two-dimensional areal coverage, its weakness in its inability to capture vegetation height. Hopefully, the present work successfully shows how they can be combined to enhance the merits of each methodology to yield wider range areal distribution of LAI so significant to and thus, much sought after for global change studies. Combination of these two different means of remote sensing can also be

applicable to many other areas of vegetation science and forestry.

### References

- Barbour, M.G. and Billings, W.D. (2000): North American Terrestrial Vegetation. 2nd ed. Cambridge, Cambridge University Press, 708 p.
- Barrett, E.C. and Curtis, L.F. (1992): Introduction to Environmental Remote Sensing. 3rd ed. London, Chapman & Hall, 426 p.
- Bolstad, P.V. and Lillesand, T.M. (1992): Improved classification of forest vegetation in Northern Wisconsin through a rule-based combination of soils, terrain, and Landsat Thematic Mapper data. *For. Sci.*, **38**, 5–20.
- Cannell, M.G.R. (1982): World Forest Biomass and Primary Production Data. London, Academic Press, 391 p.
- Chen, J.M., Rich, P.M., Gower, S.T., Norman, J.M. and Plummer, S. (1997): Leaf area index of boreal forests: Theory, techniques, and measurements. *J. Geophys. Res.*, **102**, 29429–29443.
- Cihlar, J., Beaubien, J., Xiao, Q., Chen, J.M. and Li, Z. (1997): Land cover of the BOREAS region from AVHRR and LANDSAT data. *Can. J. Remote Sensing*, **23**, 163–175.
- Cohen, W.B. and Spies, T.A. (1992): Estimating structural attributes of Douglas-fir/Western hemlock forest stands from Landsat and SPOT imagery. *Remote Sensing Environ.*, **41**, 1–17.
- Fox, L. III, Mayer, K.E. and Forbes, A.R. (1983): Classification of forest resources with Landsat data. *J. For.*, **81**, 283–287.
- Friedl, M.A. and Brodley, C.E. (1997): Decision tree classification of land cover from remotely sensed data. *Remote Sensing Environ.*, **61**, 399–409.
- Kusakabe, T., Tsuzuki, H., Hughes, G. and Sweda, T. (2000): Extensive forest leaf area survey aiming at detection of vegetation change in subarctic-boreal zone. *Polar Biosci.*, **13**, 133–146.
- Lillesand, T.M. and Kiefer, R.W. (1994): Remote Sensing and Image Interpretation. 3rd ed. New York, John Wiley & Sons, 750 p.
- Mabuchi, K., Sato, Y., Kida, H., Saigusa, N. and Oikawa, T. (1997): A Biosphere-Atmosphere Interaction Model (BAIM) and its primary verifications using glassland data. *Pap. Meteorol. Geophys.*, **47**, 115–140.
- Moore, M.M. and Bauer, M.E. (1990): Classification of forest vegetation in North-Central Minnesota using Landsat Multispectral Scanner and Thematic Mapper data. *For. Sci.*, **36**, 330–342.
- National Climatic Data Center, NOAA: web site, <http://www.ncdc.noaa.gov/ghcn/ghcn.SELECT.html>
- Nelson, R.F., Latty, R.S. and Mott, G. (1984): Classifying northern forests using Thematic Mapper simulator data. *Photogramm. Eng. Remote Sensing*, **50**, 607–617.
- Sellers, P.J. (1992): Biophysical models of land surface processes. *Climate System Modeling*, ed. by K.E. Trenberth. Cambridge, Cambridge University Press, 451–490.
- Shen, S.S., Badhwar, G.D. and Carnes, J.G. (1985): Separability of boreal forest species in the Lake Jennette area, Minnesota. *Photogramm. Eng. Remote Sensing*, **51**, 1775–1783.
- Steyaert, L.T., Hall, F.G. and Loveland, T.R. (1997): Land cover mapping, fire regeneration, and scaling studies in the Canadian boreal forest with 1 km AVHRR and Landsat TM data. *J. Geophys. Res.*, **102**, 29581–29598.
- Tsuzuki, H., Abraham, E.R.G., Kusakabe, T., Yamamoto, T. and Sweda, T. (1998): Timber cruising over extensive forest area with Airborne Laser Altimeter. *Proc. of IUFRO International Symposium on Global Concerns for Forest Resource Utilization (FORESEA)*, 746–754.
- U.S. Geological Survey and National Oceanic and Atmospheric Administration (1984): Landsat 4 Data Users Handbook. Sioux Falls, U.S. Geological Survey.
- Whittaker, R.H. and Likens, G.E. (1975): The biosphere and man. *Primary Productivity of the Biosphere*, ed. by H. Lieth and R.H. Whittaker. New York, Springer-Verlag, 305–328.
- Wolter, P.T., Mladenoff, D.J., Host, G.E. and Crow, T.R. (1995): Improved forest classification in the Northern Lake States using multi-temporal Landsat imagery. *Photogramm. Eng. Remote Sensing*, **61**, 1129–1143.

*(Received May 12, 2000; Revised manuscript accepted November 16, 2000)*